

Short communication

# Synthesis and characterization of ultrafine $\text{LiCoO}_2$ powders by a spray-drying method

Yangxing Li<sup>\*</sup>, Chunrong Wan, Yuping Wu, Changyin Jiang, Yongjun Zhu

*Institute of Nuclear Energy Technology, Tsinghua University, Beijing, 102201, China*

Received 19 January 1999; accepted 27 January 1999

## Abstract

A spray-drying method has been developed to synthesize a molecularly mixed precursor from which ultrafine  $\text{LiCoO}_2$  powder is prepared by sintering in a short time. Measurements of DTA/TGA, IR, XRD, SEM and reversible capacity are performed to characterize the properties of the prepared materials. The obtained powder is HT- $\text{LiCoO}_2$  with an  $\alpha\text{-NaFeO}_2$  structure. It is homogeneous with a grain size in the order of hundreds of nanometers. The electrochemical properties are good, viz., an initial charge capacity of  $148 \text{ mA h g}^{-1}$ , a discharge capacity of  $135 \text{ mA h g}^{-1}$ , and satisfactory cycle-life. The commercial prospects of this novel technique are promising. © 2000 Elsevier Science S.A. All rights reserved.

*Keywords:*  $\text{LiCoO}_2$ ; Lithium-ion battery; Spray-drying method

## 1. Introduction

The increasing demand for portable and cordless electronic appliances is driving the development of compact batteries [1]. Lithium-ion batteries in particular have attracted much attention [2] because of the following attributes: high output voltage, high specific energy, long cycle-life, and no memory effect.

Lithium-transition-metal-oxides, such as  $\text{LiCoO}_2$ ,  $\text{LiNiO}_2$ ,  $\text{LiMnO}_2$ ,  $\text{LiMn}_2\text{O}_4$ , and  $\text{LiV}_3\text{O}_8$ , are all high-performance cathode materials for lithium-ion batteries [3]. When concentration of lithium ions varies in a certain range, the structure and morphology of these complex compounds do not change because of the multi-valence of the transition-metal ions [4].

At present,  $\text{LiCoO}_2$  is widely used in commercial lithium-ion batteries. The compound has a layered rock-salt structure which is based on a close-packed network of oxygen atoms with  $\text{Li}^+$  and  $\text{Co}^{3+}$  ions ordering on alternating (111) planes. The traditional method for synthesizing  $\text{LiCoO}_2$  is a solid-state reaction at high temperature [5,6]. The rate-limiting step is diffusion of atoms or ions through the reactant, the intermediate and the product. Unfortunately, the activation energy for diffusion often presents a barrier for the solid-state reaction.

Many advanced chemical processes, such as the sol-gel process, spray decomposition, and precipitation and freeze-drying rotary evaporation, supercritical drying, have been evolved to prepare high-active materials of high purity and crystallinity [7–11].

In this paper, a novel technique is presented for the preparation of cathode materials for lithium-ion batteries [12]. Spray-drying, is used to produce the precursor which is sintered to give ultrafine  $\text{LiCoO}_2$  powder. The reaction mechanism is investigated by differential thermal analysis (DTA) and thermogravimetric analysis (TGA). The reaction product is characterized by means of infrared spectra, X-ray diffraction and scanning electron microscopy. Finally, an electrochemical test at constant charge-discharge current is conducted with a laboratory coin cell.

## 2. Experimental

Equivalent molar compositions of lithium acetate and cobalt acetate were dissolved in deionized water and then a quantity of polyethylene glycol (PEG) was added. The solution was dried to form a mixed precursor by means of an airflow mode spray-drying apparatus (Fig. 1) whose atomization equipment consists of a nozzle with two flows. Atomization was controlled at an air pressure of 0.1 MPa, an inlet air temperature of  $300^\circ\text{C}$ , and an exit air tempera-

<sup>\*</sup> Corresponding author.

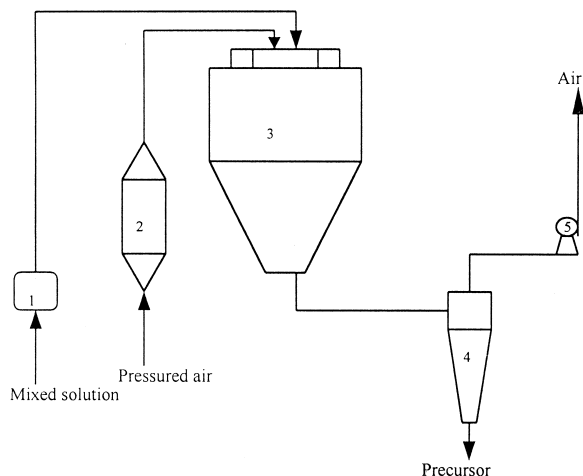


Fig. 1. Schematic of spray-drying apparatus: (1) peristaltic pump, (2) heater, (3) main tower, (4) cyclone separator, (5) fan.

ture of 100°C. Finally, the ultrafine  $\text{LiCoO}_2$  powder was synthesized by calcining the mixed precursor in air at 800°C for 4 h. A flow chart of the process is shown in Fig. 2. The entire synthesis is completed in less than 8 h.

The thermal decomposition behaviour of the mixed precursor was examined by differential thermal analysis (DTA, PCT-1) and thermogravimetric analysis (TGA, PCT-1). Infrared spectra (IR, Nicolet 560) and X-ray diffraction (XRD, D/max-RB) were used to analyze the crystalline phases of the mixed precursor and the powder. The morphology of the powder was examined by means of scanning electron microscopy (SEM, JSM-6301).

The test electrode was prepared by forming a plate which consisted of 80 wt.% active material, 10 wt.% acetylene black, and 10 wt.% polytetrafluoroethylene (PTFE). After the test electrode was dried in a vacuum

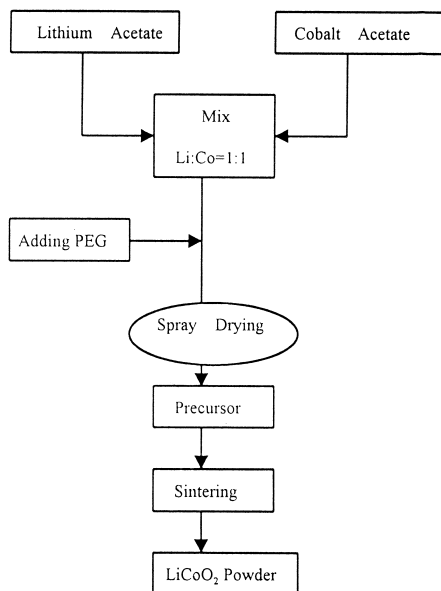


Fig. 2. Flow chart of the procedure used to synthesize  $\text{LiCoO}_2$ .

oven at 150°C for 24 h, the electrochemical performance of the active material was evaluated in a laboratory coin-type cell which contained a lithium foil anode, a separator (Celgard 2400 membrane), and an electrolyte of 1 M  $\text{LiPF}_6$  dissolved in ethylene carbonate (EC) and diethyl carbonate (DEC) (1:1). The entire cell was assembled in an argon-filled glove box. The cells were tested using a constant current density of  $0.5 \text{ mA cm}^{-2}$  in the voltage range 3.0 to 4.3 V.

### 3. Results and discussion

#### 3.1. DTA / TGA examination

The total weight loss of the precursor terminated at 300°C and four discrete regions of weight loss occurred at 180, 187, 231, and 241°C, respectively, (see Fig. 3). The thermogravimetric behaviour below 180°C represents gain and loss of the absorbing and structural water, which is accompanied by an endothermic reaction. In the temperature range 180 to 300°C, there are three obvious weight-loss peaks in the TGA curve and, at the same time, there are three intensive exothermic peaks in the DTA curve. These peaks are all associated with the combustion and decomposition of inorganic and organic constituents in the mixed precursor.

#### 3.2. IR spectra

The infrared spectra of the mixed precursor and the prepared ultrafine  $\text{LiCoO}_2$  powder are presented in Fig. 4. The spectrum of the mixed precursor (Fig. 4(a)) is the combined spectra of lithium acetate, cobalt acetate, and PEG. In fact, no chemical reactions take place during spray drying, which is confirmed by the XRD pattern of the mixed precursor (Fig. 5(a)). For  $\text{LiCoO}_2$ , the spectrum is comprised of the vibrations of the  $\text{LiO}_2$  and  $\text{CoO}_2$  layers [13]. As evident from Fig. 4(b), four bands can be resolved in the IR spectrum of  $\text{LiCoO}_2$  in the region 400 to 700  $\text{cm}^{-1}$ : three intense bands at 544, 604, and 656  $\text{cm}^{-1}$ , and one weak band at 559  $\text{cm}^{-1}$ . These bands are all attributed to  $\text{CoO}_2$  vibrations whereas  $\text{LiO}_2$  vibrations lie within the region 200 to 400  $\text{cm}^{-1}$ .

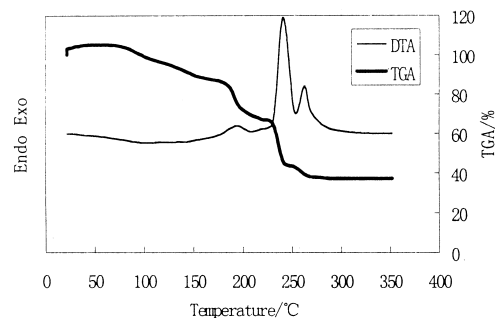


Fig. 3. DTA/TGA curves of precursor formed by spray-drying.

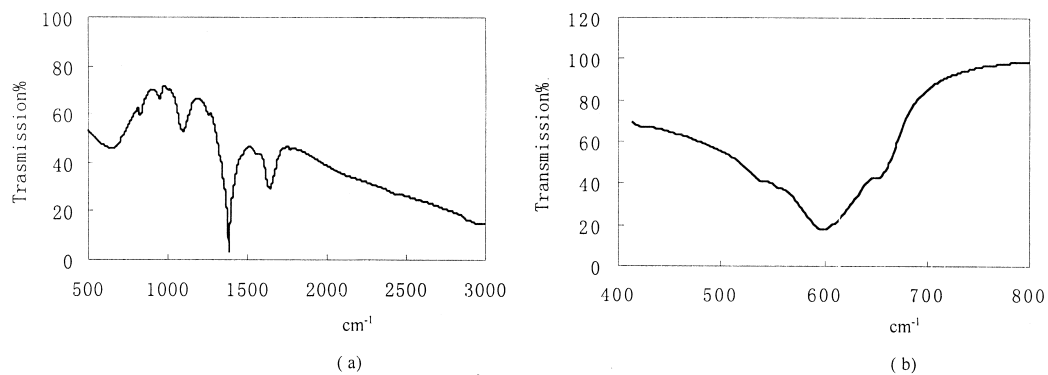


Fig. 4. IR spectra of (a) precursor, (b)  $\text{LiCoO}_2$ .

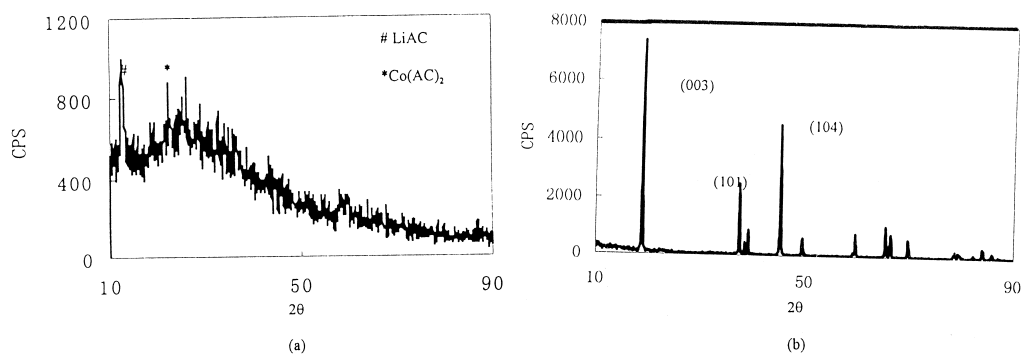


Fig. 5. XRD patterns: (a) precursor, (b)  $\text{LiCoO}_2$ .

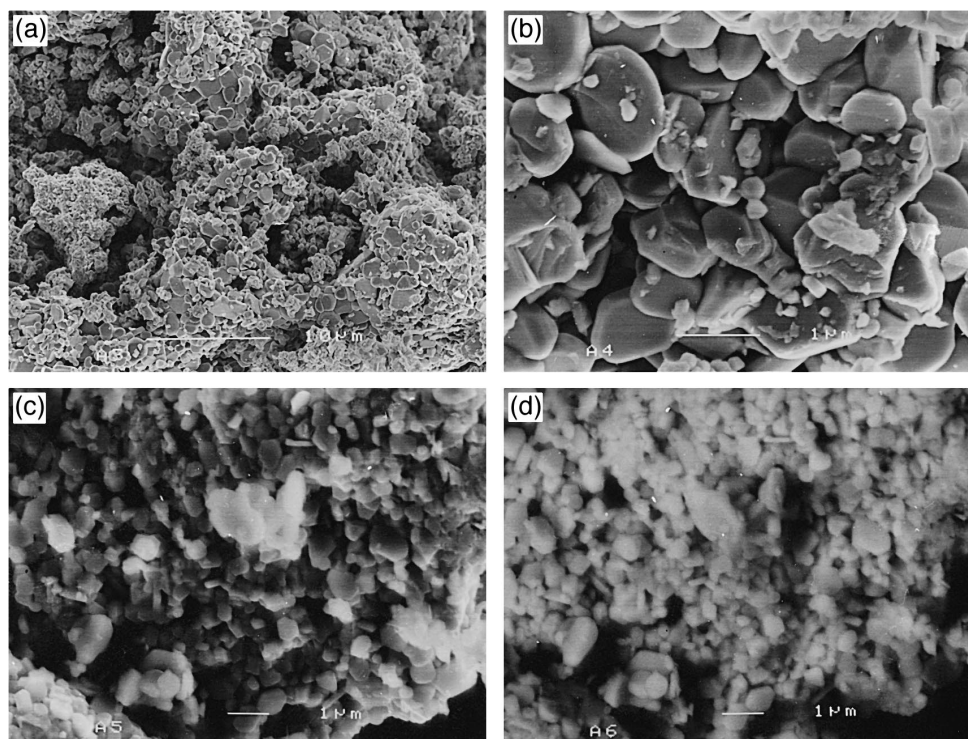


Fig. 6. Electron micrographs of ultrafine  $\text{LiCoO}_2$  powders. Servicing edition image (a)  $\times 3000$ , (b)  $\times 20000$ , (c)  $10000$ . Backscattering electron image (d)  $\times 10000$ .

### 3.3. XRD analysis

The XRD patterns of the mixed precursor and the prepared ultrafine LiCoO<sub>2</sub> powder are shown in Fig. 5. The precursor (Fig. 5(a)) is basically amorphous with a lithium acetate (011) peak at 12.78° and cobalt acetate (131) peak at 32.70°. This is in agreement with the IR spectrum. The XRD pattern (Fig. 5(b)) of the LiCoO<sub>2</sub> powder synthesized by sintering the precursor at 800°C for 4 h was indexed to HT (high temperature)-LiCoO<sub>2</sub> with a standard α-NaFeO<sub>2</sub> structure type. There are three strong peaks at 18.90° (003), 37.40° (101), and 45.24° (104). No peaks attributed to other phases are observed [14]. The fast XRD method for characterization of LiCoO<sub>2</sub> is based on the linear relationship between the *c*:*a* ratio. For a hexagonal lattice, the *c*- and *a*-parameters can be obtained from the following expressions:

$$\frac{1}{d_{hkl}^2} = \frac{4}{3} \left( \frac{h^2 + hk + k^2}{a^2} \right) + \frac{l^2}{c^2} \quad (1)$$

$$\delta_{hkl} = \frac{1}{d_{hkl}^2} - \frac{4}{3} \left( \frac{h^2 + hk + k^2}{a^2} \right) - \frac{l^2}{c^2} \quad (2)$$

$$\min = \sum_{(hkl)} \delta_{hkl}^2 \quad (3)$$

According to expression (3), the lattice parameters can be calculated accurately by the least-squares method based on the peak angles of the five stronger reflections, namely (003), (101), (006), (012) and (104). The calculated lattice parameters are *a* = 0.28152 nm and *c* = 1.40579 nm. The value denoted here as (*c*:*a*)<sub>5</sub> = 4.9900 is much higher than the ideal characteristic of a cubic lattice with a (*c*:*a*) value of 4.8990 and is consistent with a reported value of 4.989 [15]. This shows that the structure of the oxygen atoms is not an ideally-close-packed network.

### 3.4. SEM analysis

Scanning electron micrographs are shown in Fig. 6. The micrograph in Fig. 6(a) shows that the powder is uniform with a small grain size and no agglomeration. According to Fig. 6(b), the average particle size is in the range 200 to 700 nm. Fig. 6(c) and (d) are, respectively, a secondary electron image and a backscattered electron image in the same arbitrary minute area. Comparison of these two images shows that a contrast yielded by the difference in atomic number does not exist. Thus, the distribution of Li, Co, and O atoms is homogeneous.

### 3.5. Electrochemical test

An electrochemical test was conducted with a constant charge–discharge current of 0.5 mA cm<sup>-2</sup> in the voltage range 4.3 to 3.0 V. The profile (see Fig. 7) shows that the electrochemical behaviour of the powder is good with an

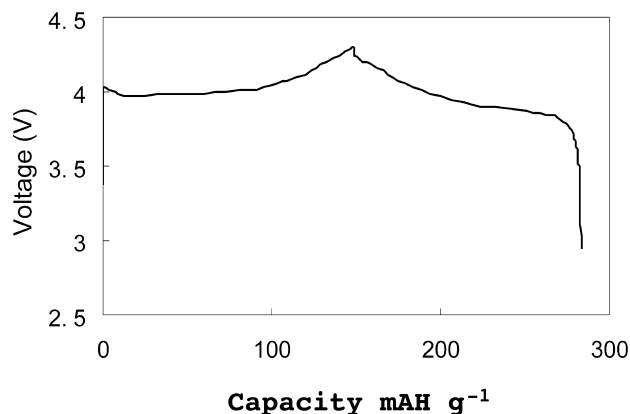


Fig. 7. Initial charge–discharge curve of LiCoO<sub>2</sub>.

initial charge capacity of 148 mA h g<sup>-1</sup> and a discharge capacity of 135 mA h g<sup>-1</sup> in the laboratory coin cell. There is a long plateau in both the charge and the discharge curve. There is no decrease in capacity over 10 cycles.

## 4. Conclusions

A spray-drying method has been developed to synthesize a molecularly mixed precursor from which an ultrafine LiCoO<sub>2</sub> powder is prepared by sintering in a short time with simple technology. The whole synthesizing process can be completed within 8 h. The powder is homogeneous and is a HT-LiCoO<sub>2</sub> phase of the α-NaFeO<sub>2</sub> structure type. An electrochemical test with constant-current charge–discharge confirms that the electrochemical property of the powder in a laboratory coin cell is good with an initial charge capacity of 148 mA h g<sup>-1</sup>, a discharge capacity of 135 mA h g<sup>-1</sup>, and a long cycle-life. There is a long plateau in both the charge and the discharge curve. In fact, this method can also be used to synthesize other cathode materials for lithium-ion batteries and has good prospects for commercialization.

## Acknowledgements

This work was supported financially in part by Materials and Analysis Fund of Tsinghua University.

## References

- [1] B. Scrosati, Nature 373 (1995) 557.
- [2] S. Megahed, W. Ebner, J. Power Sources 54 (1995) 155.
- [3] R. Koksang, J. Barker, H. Shi, M.Y. Saidi, Solid State Ionics 84 (1996) 1.
- [4] H.Q. Yang, B.Y. Sun, G.Q. Wang, N. Li, W.J. Zhang, B.X. Lin, Acta Physico-chemica Sinica 12 (1996) 716.

- [5] T. Ohuzuku, H. Komori, M. Nagayama, K. Sawai, T. Hirai, J. Ceram. Soc. Japan 100 (1992) 346.
- [6] A. Lundblad, B. Bergman, Solid State Ionics 96 (1997) 173.
- [7] Y.K. Sun, I.H. Oh, S.A. Hong, J. Mater. Sci. 31 (1996) 3617.
- [8] T. Ogihara, Y. Saito, T. Yanagawa, N. Ogata, K. Yoshida, M. Takashima, S. Yonezawa, Y. Mizuno, N. Nagata, K. Ogawa, J. Ceram. Soc. Japan 101 (1993) 1159.
- [9] P.N. Kumta, D. Gallet, A. Waghay, G.E. Bolmgren, M.P. Setter, J. Power Sources 72 (1998) 91.
- [10] Y.M. Chiang, Y.I. Jiang, H.F. Wang, D.R. Sadoway, P.X. Ye, J. Electrochem. Soc. 145 (1998) 887.
- [11] D.B. Le, W.H. Smyrl, B. Owens, S. Passerini, Patent WO96,38865 (1996).
- [12] C.R. Wan, Y.X. Li, C.Y. Jiang, CN Patent Application 98120366.3 (1998).
- [13] R. Alcantara, P. Lavela, J.L. Tirado, R. Stoyanova, E. Zhecheva, J. Solid State Chem. 134 (1997) 265.
- [14] G.G. Amatucci, J.M. Tarascon, D. Larcher, L.C. Klein, Solid State Ionics 84 (1996) 169.
- [15] R.J. Gummow, D.C. Liles, M.M. Thackeray, Mat. Res. Bull. 28 (1993) 1177.